Orbital polarization of the unoccupied states in multiferroic $LiCu_2O_2$

C. L. Chen,[1,*] K. W. Yeh,[1] D. J. Huang,[2,3,4,†] F. C. Hsu,[1,5] Y. C. Lee,[1,5] S. W. Huang,[2,4] G. Y. Guo,[6] H.-J. Lin,[2] S. M. Rao,[1] and M. K. Wu[1]

[1]*Institute of Physics, Academia Sinica, Taipei 11529, Taiwan*
[2]*National Synchrotron Radiation Research Center, Hsinchu 30076, Taiwan*
[3]*Department of Physics, National Tsing Hua University, Hsinchu 30013, Taiwan*
[4]*Department of Electrophysics, National Chiao Tung University, Hsinchu 30010, Taiwan*
[5]*Department of Materials Science and Engineering, National Tsing Hua University, Hsinchu 30013, Taiwan*
[6]*Department of Physics, National Taiwan University, Taipei 10617, Taiwan*

(Received 8 August 2008; revised manuscript received 22 October 2008; published 12 December 2008)

Using measurements of polarization-dependent soft-x-ray absorption and band-structure calculations including the on-site Coulomb interaction, we investigated the symmetry of the intrinsic 3*d* holes in the low-dimensional quantum magnet $LiCu_2O_2$ with edge-sharing spin chains. The Cu *L*-edge and O *K*-edge measurements with in-plane and out-of-plane **E** vectors of x ray reveal the orbital character of the valence states of Cu on different sites. The unoccupied 3*d* states of nominal Cu^{2+} exhibit predominantly *xy* symmetry, whereas 3*d* holes of $3z^2-r^2$ symmetry reside on the nominal Cu^+ sites. Both the experimental observations and theoretical calculations agree on the hybridization of the O 2*p* and Cu 3*d* states above the Fermi level. The existence of 3*d* holes on Cu^+ enhances the interlayer magnetic coupling.

DOI: 10.1103/PhysRevB.78.214105 PACS number(s): 71.20.Be, 78.70.Dm, 73.20.At

I. INTRODUCTION

Low-dimensional quantum spin systems with geometric frustration have attracted much attention for decades. One-dimensional CuO chains with a Cu-O-Cu bond angle of 180° as found in Sr_2CuO_3 and $SrCuO_3$ are antiferromagnets which exhibit strong quantum spin fluctuations. Similarly, compounds of edge-sharing CuO_2 chains with the Cu-O-Cu bond angle of about 90° such as $LiCu_2O_2$ are frustrated magnets because of competition between ferromagnetic (FM) and antiferromagnetic (AFM) exchanges and, thus, exhibit rich magnetic phases. $LiCu_2O_2$ is also important for studying interesting spin-lattice interaction, magnetic ordering, quantum spin correlations, and specific heat of a spin-$\frac{1}{2}$ quantum antiferromagnet with spin spirals.[1–6] Its low dimensionality and quantum spin fluctuations lead to profound and intriguing effects on magnetic and electronic properties. For example, Pisarev *et al.*[7] observed an anomalous optical spectral feature which thoroughly disagrees with *ab initio* calculations. Masuda *et al.*,[1] using neutron diffraction, found that the spin structure of $LiCu_2O_2$ is helimagnetic. Local-density-approximation-based calculations of exchange integrals also reveal a large in-chain frustration leading to a spin spiral.[2] Based on data of angle-resolved photoemission and optical measurements, Papagno *et al.*[3] suggested a one-dimensional scenario of strongly correlated antiferromagnetic insulators for $LiCu_2O_2$; however, results of soft-x-ray magnetic scattering by Huang *et al.*[4] imply a quasi-two-dimensional magnetic order.

Recently, $LiCu_2O_2$ has been found to be a member of cuprate multiferroics in which magnetism and ferroelectricity coexist and ferroelectric polarization can be reversibly flipped with an applied magnetic field.[5,6,8,9] Of particular interest is how the induced electric polarization by magnetism can survive out of quantum fluctuations. The magnetic structure in the ferroelectric ground state of $LiCu_2O_2$ is still perplexing.[5,6,10–12] Density-functional calculations of electric polarizations by Xiang and Whangbo[10] show that the observed spin-spiral plane is inconsistent with the observed direction of the electric polarization. In additional, Moskvin and Drechsler[11] concluded that, in the scenario of spin current, the induced polarization due to two consecutive CuO_4 plaquettes along the chain gets canceled exactly, and the *c*-axis coupling of spins are essential for the observed multiferrocity,[12] supported by measurements of soft-x-ray magnetic scattering.[4]

$LiCu_2O_2$ also represents a useful starting point to obtain basic information relevant to complex behavior displayed by transition-metal compounds. It is a mixed-valence compound with a layered orthorhombic crystal structure of the space group *Pnma* ($Z=4$), lattice parameters $a=5.72$ Å, $b=2.860$ Å, and $c=12.399$ Å. This compound has an equal number of nominal Cu^{2+} and Cu^+ oxidation states. Cu^{2+} ions are magnetic and located at the center of the square base of a fivefold oxygen pyramid with an apical oxygen. Quasi-one-dimensional chains of magnetic order develop along the *b* axis with CuO_4 plaquettes in which the Cu-O-Cu bonding angle is 94°. Two adjacent Cu^{2+} ions in the CuO_4 plaquette are labeled as Cu(3) and Cu(4), as shown in Fig. 1. Double layers of Cu^{2+} stack along the *c* direction with intervened layers of nonmagnetic Cu^+ ions, which are labeled as Cu(1) and Cu(2). This edge-sharing cuprate $LiCu_2O_2$ is a unique and simple model system for testing theories of spin correlations in frustrated quantum magnets.

Revealing the underlying mechanism of physical properties of $LiCu_2O_2$ such as quantum multiferroic features requires a full understanding of the electronic structure involved with magnetic coupling, particularly the orbital polarization and the *p-d* hybridization in the unoccupied states. Several experiments and theories indicate that $LiCu_2O_2$ exhibits strong electron-hole correlations of coppers on different sites[7] and that Cu^{2+} possesses characteristics of *p-d* hybridization in the *ab* plane. In contrast, non-

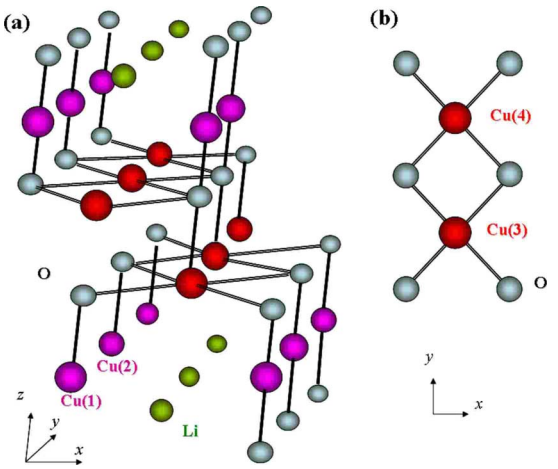

FIG. 1. (Color online) (a) Illustration of the crystal structure of $LiCu_2O_2$. Cyan balls stand for oxygen. Li ions are denoted by green balls. Purple and red balls represent the monovalent and divalent copper ions, respectively. (b) Two-dimensional (2D) view of the edge-sharing chain along the y axis, i.e., the b axis. Adjacent Cu^{2+} ions along the chain are labeled Cu(3) and Cu(4); Cu^{+} ions are labeled Cu(1) and Cu(2) which bridge the double layers of Cu^{2+}.

magnetic ions Cu^{+} in the linear bonding of O-Cu-O along the c axis are expected to exhibit fully occupied $3d$ orbitals.[3,7,13]

X-ray absorption spectroscopy (XAS) provides information on the symmetry of the unoccupied electronic states. The absorption cross section of x ray depends on the direction of the **E** vector with respect to the crystallographic orientations and the orbital orientation of unoccupied electronic states of transition-metal $3d$ and oxygen $2p$. XAS with linearly polarized x ray yields a characterization of the orbital orientation of the unoccupied states.[14,15] Here, we present measurements of polarization-dependent Cu L-edge and O K-edge XAS to understand the electronic structure derived from Cu^{2+} and Cu^{+}. Band-structure calculations in the scheme of generalized gradient approximation (GGA) (Ref. 16) with the on-site Coulomb interaction U taken into account,[17] i.e., GGA+U calculations, are also presented to interpret the XAS results. We discuss the orbital polarization of unoccupied electronic states derived from Cu^{2+} and Cu^{+}.

II. EXPERIMENTAL

Single crystals of $LiCu_2O_2$ were grown by the floating zone technique in which the oxygen atmosphere was well controlled to stabilize the $LiCu_2O_2$ phase by reducing the Cu loss that occurs typically in the growth by the self-fluxing technique.[1] Characterization of x-ray diffraction indicates that the $LiCu_2O_2$ samples exhibit a good crystalline structure and are free of impurity phases such as Li_2CuO_2, $LiCu_3O_3$, and CuO. The x-ray Laue pattern shows that (not shown here) the crystals were discovered to be twinned at [110] plane with a mixing of the a- and b-axis domains as observed previously in the literature.[1,4–6,18]

Polarization-dependent x-ray absorption spectra were recorded at the Dragon (11A1) beamline of the National Synchrotron Radiation Reach Center (NSRRC) in Taiwan. To obtain XAS spectra containing the evolution from $\mathbf{E} \perp \hat{c}$ to $\mathbf{E} \| \hat{c}$, we measured XAS of Cu L and O K edges with the total electron yield method under various incidence angles θ between the incident photon beam and the surface normal $\hat{c}$ of crystal, i.e., the crystallographic c axis. The energy resolutions are 0.15 and 0.4 eV in the O K-edge and Cu L-edge regions, respectively. All XAS measurements of different crystal orientations are normalized to have an equal XAS intensity at 40 and 70 eV above the Cu L and O K edges, respectively. Standard oxide powders of CuO and Cu_2O are used for energy calibration and also for comparing different electronic valence states.

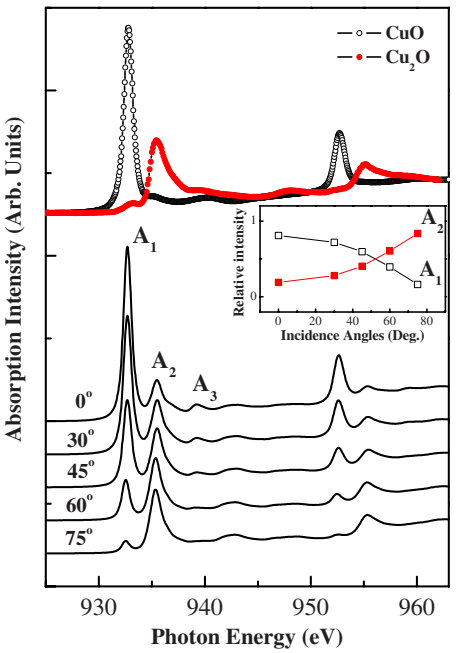

FIG. 2. (Color online) XAS spectra of Cu $2p_{3/2}$ (L_3) and $2p_{1/2}$ (L_2) absorption edges of $LiCu_2O_2$ for different orientations of the **E** x ray. θ is the incidence angle between the incident photon beam and the surface normal $\hat{c}$ of crystal, i.e., the crystallographic c axis. The origins of XAS features A_1, A_2, and A_3 are discussed in the text. The inset shows the relative intensities of A_1 and A_2 as a function of θ.

III. RESULTS AND DISCUSSION

Figure 2 shows Cu L-edge XAS spectra obtained with various incidence angles θ. The spectra stem from excitations of a core electron in the $2p_{1/2}$ or $2p_{3/2}$ manifold to the unoccupied $3d$ state, i.e., transitions from a ground state of $2p^6 3d^n$ to an excited electronic configuration of $2p^5 3d^{n+1}$ with different multiplet excitations. As a result of spin-orbit coupling in the $2p$ state, the spectra display two prominent features in the energy ranges of 931–939 and 951–959 eV, respectively, corresponding to the L_3 ($2p_{3/2} \rightarrow 3d$) and L_2 ($2p_{1/2} \rightarrow 3d$) absorptions. Because of the change in the incidence angle, Fig. 2 provides the evolution of XAS with the electric-field vector **E** from being parallel to being perpendicular to the c axis. Two main anisotropic peaks marked as A_1 and A_2 dominate the features of spectral evolution about

the L_3-edge absorption. Comparing the divalent and monovalent oxidation states of Cu with different symmetries, one can identify the valence states from the evolution of the absorption spectra. The ground state of the nominal Cu^{2+} is a hybridization of $3d^9$ and $3d^{10}\underline{L}$, where $\underline{L}$ denotes a hole in the O $2p$ valence band, i.e., the $2p$ ligand hole. The sharp peak A_1 centered at photon energy 932.7 eV in the L_3-edge absorption arises from the $2p^63d^9 \rightarrow 2p^53d^{10}$ transition of Cu^{2+}, such as that of Cu^{2+} in CuO.[19] The effective screening by the core-hole potential in the XAS final state gives rise to the observed sharp resonance of A_1. On the contrary, A_2 stands out in the XAS geometry close to $\mathbf{E}\|\hat{c}$ at an energy almost identical to that of Cu^+ in Cu_2O which exhibits a combination of $3d^{10}$, $3d^94s^1$, and $3d^{10}4s^1\underline{L}$ in the ground state.[19–21] Such a broad feature of A_2 originates from a d^9-like ground state. A weak feature of A_3 also appears at 939.2 eV, as a contribution from the $3d^{10}\underline{L}$ configuration in the ground state, which has the $p_{x,y}$ bonding state.[22,23]

Our XAS data show that the ground state of Cu^+ contains the electronic configuration $3d^94s^1$. This observation of $3d$ hole Cu^+ does not result from a nonstoichiometric effect. Masuda *et al.*[1] found that a chemical disorder and a Cu deficiency are inherently present in $LiCu_2O_2$. The excess Li^+ ions occupy Cu^{2+} sites due to a good match of ionic radii. The charge compensation requires that the introduction of Li^+ ions into the double chains of Cu^{2+} is accompanied by a transfer of the holes onto the Cu^+ interchain sites. However, the energy of the observed XAS feature in A_2 coincides with that of the nominal Cu^+ in Cu_2O rather than the divalent Cu^{2+} in CuO. XAS results hence indicate that intrinsic $3d$ holes do exist on the nominal Cu^+ sites regardless of nonstoichiometry, in contrast to the intuitive expectation of $3d^{10}$ configuration.

The polarization-dependent XAS measurements reveal that, when the absorption geometry evolves from $\mathbf{E}\perp\hat{c}$ toward $\mathbf{E}\|\hat{c}$, the intensity of A_1 decreases, whereas the XAS feature of A_2 is enhanced strongly, as further illustrated in the inset of Fig. 2. The intensity of A_3 also gradually decreases as the absorption geometry changes accordingly. These XAS data thus show that the unoccupied $3d$ state on Cu^{2+} has an in-plane orbital polarization. In other words, the evolution of A_1 unravels the in-plane character of the unoccupied $3d_{xy}$ orbital of Cu^{2+} in the CuO_4 plaquettes running along the b axis. The feature of A_2, on the other hand, is dominated by the z character from the d^9-like ground state of Cu^+ as confirmed by the O K-edge spectra that will be discussed later. In addition, the XAS feature of A_2 remains finite even with $\mathbf{E}\perp\hat{c}$, such as that of Cu_2O in which the XAS final state is mainly of $2p^53d^{10}4s^1$. These spectra therefore indicate that the observed peak A_2 consists of two transitions which reach the XAS final state of Cu^+. First, there occurs a transition of $2p^63d^94s^1 \rightarrow 2p^53d^{10}4s^1$ involved with a $3d_{3z^2-r^2}$ hole in the ground state. The other is the $2p^63d^{10} \rightarrow 2p^53d^{10}4s^1$ transition in which the XAS intensity is independent of the orientation of $\mathbf{E}$ because of the isotropic nature of the $4s$ state.

To further understand the orbital symmetry of $3d$ states in $LiCu_2O_2$, we performed GGA+U (Ref. 17) electronic structure calculations. Coulomb energy U=4.5 eV and exchange parameter J=0.9 eV for all Cu atoms were adopted. We used the highly accurate all-electron full-potential linearized augmented plane-wave (FLAPW) method, as implemented in WIEN2K package.[24] The experimental structural parameters with lattice constants a=5.7260 Å, b=2.8587 Å, and c=12.4137 Å (Ref. 25) were used. We considered the simple collinear AFM structure with the $1\times2\times1$ supercell and found that the AFM $LiCu_2O_2$ is a semiconductor with a band gap of 0.94 eV. As expected, Cu^+ ions [Cu(1) and Cu(2)] have a negligible spin magnetic moment ($<0.001\mu_B$/atom). Nevertheless, Cu^{2+} ions [Cu(3) and Cu(4)] have a spin magnetic moment of $\sim0.65\mu_B$/atom (not $\sim1.0\mu_B$/atom), in agreement with previous LSDA+U calculations.[13]

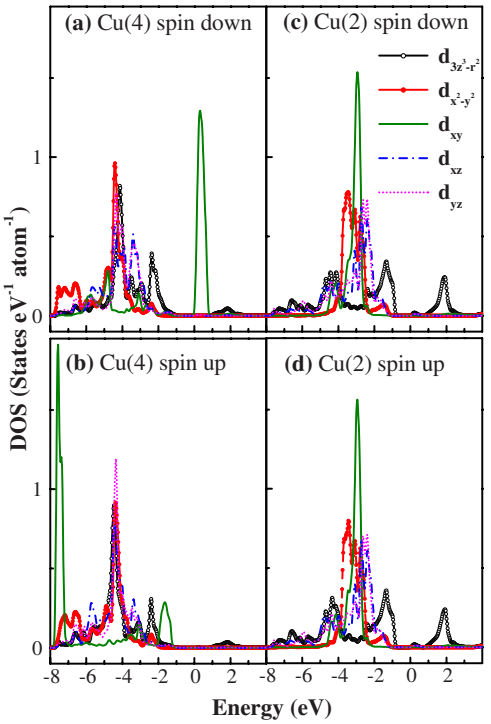

FIG. 3. (Color online) Density of states of $LiCu_2O_2$ in the antiferromagnetic state obtained from GGA+U band-structure calculation. (a)–(d) are plots of the d-decomposed DOS of Cu on different sites. The E_F is located at the energy equal to zero in all the spectra.

Figure 3 plots the decomposed partial density of states (DOS) of Cu^{2+} and Cu^+ on different Cu sites from GGA+U calculations. Figures 3(a) and 3(b) show the calculated spin-down and spin-up DOSs of Cu(4) for divalent Cu^{2+}, respectively; Figs. 3(c) and 3(d) show the spin-down and spin-up DOSs for monovalent Cu^+, respectively. Note that the spin-up DOS of Cu(4) and spin down of Cu(3) are identical because of the antiferromagnetic order set in the calculations. The calculations indicate that Cu^{2+} on the Cu(4) sites has a spin-down $3d_{xy}$ state at 0.32 eV above the Fermi level (E_F). In addition, Cu^{2+} on both Cu(3) and Cu(4) sites have a weak nonmagnetic $3d_{3z^2-r^2}$ state at 1.87 eV. There also exist $3d$ holes of $d_{3z^2-r^2}$ symmetry on Cu^+ at 1.90 eV on both Cu(1) and Cu(2) sites, as shown in Figs. 3(c) and 3(d). The above observations of Cu L-edge XAS and GGA+U calculations lead us to conclude that there exist unoccupied $3d$ states on the nominal Cu^+ sites in $LiCu_2O_2$ to mediate the magnetic coupling between successive double-layered CuO_4

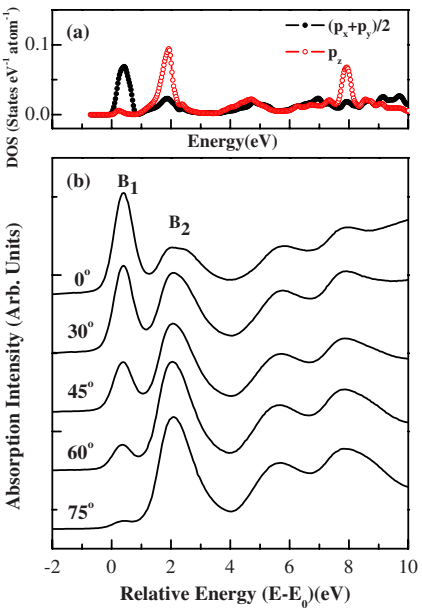

FIG. 4. (Color online) (a) *p*-decomposed density of states of $LiCu_2O_2$ from GGA+*U* band-structure calculations. (b) O *K*-edge XAS of $LiCu_2O_2$ for the electronic field vector **E** from being parallel to perpendicular to the surface normal (exact angle value depending on θ). The relative energy denoted in (b) is aligned with the absorption energy of O *K* edge in such a way that the first peak of the DOS in (a) coincides with peak B_1. The relative zero energy in (b) corresponds to the photon energy of 529.3 eV in the O *K*-edge XAS.

plaquettes. Such a weakly magnetic coupling along the *c* axis is through the $3d_{3z^2-r^2}$ orbitals of Cu^+. Furthermore, as will be discussed later, the energies of O 2*p* unoccupied states above the Fermi level shown in Fig. 4(a) coincide with those of Cu, evidencing the *p*-*d* hybridization.

Figure 4(a) displays the O 2*p* DOS projected onto the directions perpendicular and parallel to the *c* axis. The scale of relative energy denoted in Fig. 4(a) is aligned with the O *K*-edge data in such a way that the first peak of the DOS coincides with the B_1 peak of Fig. 4(b). The prediction of the *p*-*d* hybridization from GGA+*U* calculations is also corroborated by the measurements of O *K*-edge absorption, a dipole-allowed transition from O 1*s*- to 2*p*-derived unoccupied states. The threshold structures observed near the O *K*-edge XAS are determined by the electronic structure of Cu 3*d* because of the ground-state hybridization between Cu 3*d* and O 2*p*. Hence O *K*-edge absorption can be interpreted in a similar way as the one-electron addition of Cu 3*d*, such as the bremsstrahlung isochromat spectroscopy. The near-edge structure of O $1s \rightarrow 2p$ absorption provides a measure of the partial density of states projected onto the O 2*p* states. Figure 4(b) shows the polarization-dependent O *K*-edge XAS of $LiCu_2O_2$ with various incidence angles. These XAS spectra display several prominent features of the oxygen 2*p* bands. As the XAS geometry changes from the in-plane to out-of-plane **E** vectors, the intensity of the lowest-energy absorption marked as B_1 decreases and the XAS of 2 eV above marked B_2 is enhanced, such as the evolution of the Cu *L*-edge XAS. The features of B_1 and B_2 result from the transitions of 1*s* to 2*p* states hybridized with 3*d* of Cu^{2+} and Cu^+, respectively.[19,20] Peak B_1 is from the contribution of the unoccupied O 2*p* hybridized with 3*d* states of *xy* symmetry on Cu^{2+} which form the upper Hubbard band (UHB).[26] In contrast, B_2 is from those hybridized with 3*d* of Cu^+ in which the ground state is a combination of $3d^{10}$ and $3d^9 4s^1$. Consequently, the 2*p* bands exhibit both *z* and *xy* characters that exist, consistent with GGA+*U* calculations; even a small splitting of B_2 measured with the in-plane geometry can be explained by the calculations. Note that we performed GGA+*U* calculations with several different values of Coulomb interaction energy, i.e., $U=0.0$, 3.0, 4.5, 6.0, and 7.0 eV. However, we found that good agreement between the O *K*-edge XAS and O 2*p*-orbital-decomposed DOS (Fig. 4) is obtained only when $U=4.5$ eV.

One can link our results to the mechanism of the magnetoelectric coupling in $LiCu_2O_2$. At first sight, arising of the induced polarization **P** in $LiCu_2O_2$ seems to be best understood in terms of the spin-current model[27] or the inverse Dzyaloshinskii-Moriya interaction,[28] where **P** is induced by two neighboring spins $\mathbf{S}_i$ and $\mathbf{S}_j$ on the chain and is determined by $\mathbf{S}_i \times \mathbf{S}_j$. Although neutron results indicated that the spin-chain structure of $LiCu_2O_2$ is spiral,[1] experimentally, conflicting results were reported regarding the magnetic structure and its relation to the observed **P** in $LiCu_2O_2$.[1,5,6] Whether the spiral spins lie on the *ab* or *bc* plane remains controversial,[1,6] while the spin-current model requires spiral spins lying on the *bc* plane to generate the observed ferroelectricity along the *c* axis. Although the true mechanism of the observed multiferroic features is not fully understood yet, the *c*-axis coupling of spins might be essential for the observed multiferrocity.[4,12] The existence of 3*d* holes on the Cu^+ site enhances the interlayer magnetic coupling along the *c* axis and seems to support such a scenario. In other words, the interlayer magnetic coupling via the 3*d* holes of Cu^+ could play a role in the induction of electric polarization.

In summary, our results reveal the symmetry of the 3*d* holes in the low-dimensional quantum magnet $LiCu_2O_2$ with edge-sharing spin chains. XAS measurements show that 3*d* holes exist not only on the Cu^{2+} sites with $3d^9$ electronic configuration but also on the Cu^+ sites which bridge layers of CuO_4 plaquettes. The nominal Cu^{2+} exhibits predominantly $3d_{xy}$ symmetry in the unoccupied states. We also found that there exist $3d_{3z^2-r^2}$ holes residing on the Cu^+ site and the hybridization between O 2*p* and Cu 3*d* states above the Fermi level. These findings indicate that the 3*d* holes of Cu^+ enhances the magnetic coupling between double layers of Cu^{2+} along the *c* axis.

ACKNOWLEDGMENTS

This work was supported by the National Science Council of Taiwan under Contract No. NSC-96-2112-M-001-026-MY3. We acknowledge the excellent technical support from the NSRRC technical staff, particularly, F. S. Chang, the manager of the Dragon beamline. We also thank the members of the Electronic and Atomic Structure Laboratory of Tamkang University for their help during XAS measurements.

*clchen@phys.sinica.edu.tw
†djhuang@nsrrc.org.tw

[1] T. Masuda, A. Zheludev, A. Bush, M. Markina, and A. Vasiliev, Phys. Rev. Lett. **92**, 177201 (2004); **94**, 039706 (2005).
[2] A. A. Gippius, E. N. Morozova, A. S. Moskvin, A. V. Zalessky, A. A. Bush, M. Baenitz, H. Rosner, and S.-L. Drechsler, Phys. Rev. B **70**, 020406(R) (2004)
[3] M. Papagno, D. Pacilé, G. Caimi, H. Berger, L. Degiorgi, and M. Grioni, Phys. Rev. B **73**, 115120 (2006).
[4] S. W. Huang, D. J. Huang, J. Okamoto, C. Y. Mou, W. B. Wu, K. W. Yeh, C. L. Chen, M. K. Wu, H. C. Hsu, F. C. Chou, and C. T. Chen, Phys. Rev. Lett. **101**, 077205 (2008); Solid State Commun. **147**, 234 (2008).
[5] S. Park, Y. J. Choi, C. L. Zhang, and S.-W. Cheong, Phys. Rev. Lett. **98**, 057601 (2007).
[6] S. Seki, Y. Yamasaki, M. Soda, M. Matsuura, K. Hirota, and Y. Tokura, Phys. Rev. Lett. **100**, 127201 (2008).
[7] R. V. Pisarev, A. S. Moskvin, A. M. Kalashnikova, A. A. Bush, and Th. Rasing, Phys. Rev. B **74**, 132509 (2006).
[8] T. Kimura, T. Goto, H. Shintani, K. Ishizaka, T. Arima, and Y. Tokura, Nature (London) **426**, 55 (2003).
[9] S.-W. Cheong and M. Mostovoy, Nature Mater. **6**, 13 (2007).
[10] H. J. Xiang and M.-H. Whangbo, Phys. Rev. Lett. **99**, 257203 (2007).
[11] A. S. Moskvin and S.-L. Drechsler, Phys. Rev. B **78**, 024102 (2008).
[12] A. S. Moskvin, Yu. D. Panov, and S.-L. Drechsler, arXiv:0801.1975 (unpublished).
[13] D. A. Zatsepin, V. R. Galakhov, M. A. Korotin, V. V. Fedorenko, E. Z. Kurmaev, S. Bartkowski, M. Neumann, and R. Berger, Phys. Rev. B **57**, 4377 (1998).
[14] C. T. Chen, L. H. Tjeng, J. Kwo, H. L. Kao, P. Rudolf, F. Sette, and R. M. Fleming, Phys. Rev. Lett. **68**, 2543 (1992).
[15] W. B. Wu, D. J. Huang, J. Okamoto, A. Tanaka, H.-J. Lin, F. C. Chou, A. Fujimori, and C. T. Chen, Phys. Rev. Lett. **94**, 146402 (2005).
[16] J. P. Perdew, K. Burke, and M. Ernzerhof, Phys. Rev. Lett. **77**, 3865 (1996).
[17] A. I. Liechtenstein, V. I. Anisimov, and J. Zaanen, Phys. Rev. B **52**, R5467 (1995).
[18] B. Roessli, U. Staub, A. Amato, D. Herlach, P. Pattison, K. Sablina, and G. A. Petrakovskii, Physica B **296**, 306 (2001).
[19] L. H. Tjeng, C. T. Chen, and S.-W. Cheong, Phys. Rev. B **45**, 8205 (1992).
[20] M. Grioni, J. F. van Acker, M. T. Czyžyk, and J. C. Fuggle, Phys. Rev. B **45**, 3309 (1992).
[21] M. Finazzi, G. Ghiringhelli, O. Tjernberg, Ph. Ohresser, and N. B. Brookes, Phys. Rev. B **61**, 4629 (2000).
[22] M. A. van Veenendaal and G. A. Sawatzky, Phys. Rev. B **49**, 3473 (1994).
[23] H. Eskes, L. H. Tjeng, and G. A. Sawatzky, Phys. Rev. B **41**, 288 (1990).
[24] P. Blaha, K. Schwarz, G. K. H. Madsen, D. Kvasnicka, and J. Luitz, *WIEN2k, An Augmented Plane Wave Local Orbitals Program for Calculating Crystal Properties* (Technische Universität Wien, Vienna, Austria, 2002).
[25] R. Berger, P. Önnerud, and R. Tellgren, J. Alloys Compd. **184**, 315 (1992).
[26] J. Fink, N. Nücker, E. Pellegrin, H. Romberg, M. Alexander, and M. Knupfer, J. Electron Spectrosc. Relat. Phenom. **66**, 395 (1994).
[27] H. Katsura, N. Nagaosa, and A. V. Balatsky, Phys. Rev. Lett. **95**, 057205 (2005).
[28] I. A. Sergienko and E. Dagotto, Phys. Rev. B **73**, 094434 (2006).